Chapter 8 Low Temperature Synthesized Sn Doped Indium Oxide Nanowires

8.0 Preface

The selective, well controlled and directionally grown Sn doped In_2O_3 nanowires (In_2O_3: Sn nanowires, SIO NWs) were synthesized at a low fabrication temperature (~770 ^oC) through a vapor-liquid-solid (VLS) process under a precise carrier gas flow. The majority of SIO NWs is grown along [222] with [400] and [440] minority forming directions which i mplies a nearly epitaxial crystal structure. There are less physical defects such as line or planar defect and contaminations in the SIO NWs through high resolution transmission electron microscopy (HR-TEM) observations. The spectrum of photoluminescence (PL) emission indicates a stable strong blue light peak located at ~440 nm while the excited wavelength is 275 nm at room temperature. The Sn dopant in the SIO NWs can enhance the conductivity of the nanowires leading to the lowering of the turn-on electric-field to 0.66 V/μm under a current density of up to 1.0 mA/cm^2 based on their field emission characteristics. Furthermore, the field emission enhancement coefficient, β is also increased to 1.48×10^5 which is very close to the carbon nanotubes, (CNTs) level. The SIO NWs fabricated by a VLS process offers a potential application in flat display as demonstrated in this study.

8.1 Introducation

Recently, much progress in the synthesis of metal oxide nanowires (especially II-VI semiconductor materials) has been driven by the requirement to explain the novel physical and optical properties of one and two dimensional nanostructures such as nanorods, nanobelts, or nanowires (NWs), and nano films. Furthermore, their potential applications in constructing nanoscale electronic and optoelectronic devices are equally subjected to more attention. The wide band gap transparent conductor material, indium oxide (In_2O_3;IO) has a direct band gap of ~3.6 eV and an indirect band gap of ~2.6 eV, which has been studied to be used in the micro electronic fields[283]. However, previous research is mainly focused on the applications of films or patricles[284-285]. The investigation of nanowires (1D nanostructure) of IO is still quite limited[286-287]. The fabrication processes have been reported for the synthesis of IO NWs are thermal evaporation and electro-deposition and oxidation. On the basis of our previous study[288-289], vapor-liquid-solid (VLS) process as able to offer improved stability and large area growth of nanowires on Si substrates under easily tunable controlled conditions. In the present, VLS method is employed to synthesize IO NWs and their field emission properties are studied. In order to promote the electronic conductivity and lower the turn-on electric field for field emission (FE) characteristic, the SnO_2 powders were added into the pure IO source powders in the VLS process that would lead to the diffusion of Sn into the IO NWs. The morphology and crystal structure of the Sn doped IO NWs (SIO NWs) are also investigated.

8.2 Experimental

A Radio Corporation of America (RCA) cleaning method was used to clean p-type Si (100) substrate. This process can remove the native oxide (~20 Å) from the surface of Si substrate. After the cleaning procedure, the 70 Å thick Au film with a diameter of 100 μm was formed on Si (100) substrate by rf-sputtering (13.56 MHz) under 10 mTorr Ar atmosphere at a power level of 30 W for 15s and then patterned by the shadow mask process. This Au film acts as a catalyst for SIO NWs synthesized through a precise carrier gas flow-controlled VLS process and the control of the growth region of the nanowires.

The source material for SIO NWs was a mixture of IO (99.998%), SnO_2 (99.98%), and graphite (99.98%) powders at a mole ratio of 0.9:0.1:1.0. The mixed powders were put on the quartz boat in front of the Au/Si substrate loaded in a horizontal alumina tube furnace. The SIO NWs were synthesized by the VLS process with the temperatures varying from 770 to 950 ^{o}C. The furnace was heated at a rate of 150 ^{o}C/min. under the gas flow rate of high purity N_2 (99.998%) varied from 20.0 to 100.0 cm^3/sec. The optimized gas flowing rate used in our study was 60.0 cm^3/sec. On the basis of our previous study[7], the carrier gas controlled to nearly laminar flow mode in the horizontal furnace is able to be helpful in the vertical growth of the nanowires. The crystal structure of the nanowires was studied by X-ray diffraction (XRD, MAC Science, MXP18, Japan). The morphology and microstructures of the SIO NWs were analyzed by field emission scanning electron microscopy (FE-SEM, Hitachi S-4700I, Japan) and high resolution transmission electron microscopy

(HRTEM, Philips tecani-20, U.S.A.). The chemical composition of nanowires was characterized by X-ray Photoelectron Spectroscopy (XPS, VG Scientific Microlab 250, UK). A photoluminescence analyzer (PL, Hitachi F-4500, Japan) with Xe lamp as an excitation source (275 nm) was used for the optical studies at room temperature. The high voltage-current instrument, Keithley 237, was used to analyze the FE characteristic of the SIO NWs. A tungsten tip probe and a controllable sample stage were all loaded in a high vacuum chamber kept under 10^{-8} Torr in the FE measurement.

8.3 Results and Discussion

The XRD patterns shown in Fig. 8.1(a) indicate the influence of growth temperature on the crystallinity of the SIO NWs. While the growth temperature is getting lower from 900 ^{o}C to 770 ^{o}C, the intensities of XRD peaks such as (222), (400), and (440) of SIO NWs[290] are getting stronger. Bsaed on SEM observations (not shown here), the nanowire density, which may also affect the peak height, does not show difference among various temperature grown SIO NWs. The relation of full-width at half-maximum (FWHM) v.s. growth temperature is shown in Fig. 8.1(b). The FWHM value decreases with a decrease in synthesized temperature from 900 to 770 ^{o}C. While the synthesized temperature is lowered to 750 ^{o}C or below, the SIO NWs were unable to be successfully grown at those temperatures. That means if the growth temperature is too low ($\leqq$750 ^{o}C), the suitable amount vapor of In or Sn is hardly formed and as a result it is difficult to carry the VLS process out. On the other hand, at such a low temperature, it does not provide enough energy to crystallize the SIO NWs. It indicated in Fig. 8.1(a) that very weak diffraction

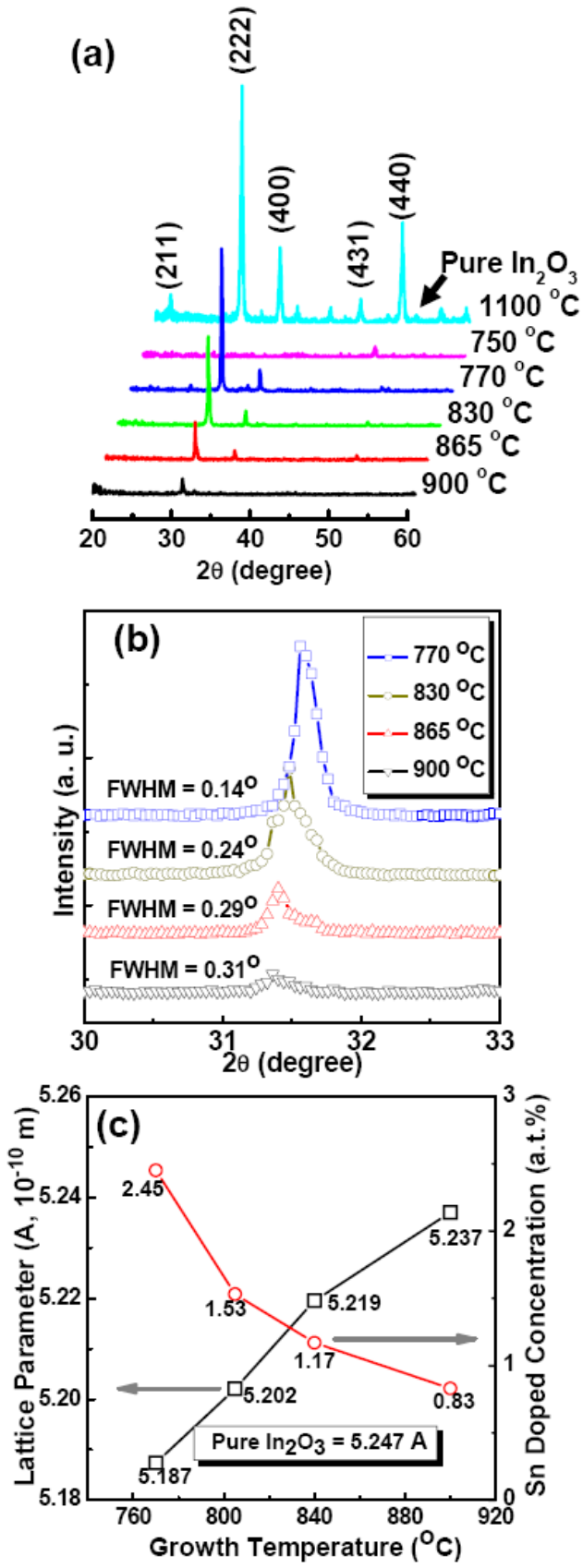

Figure 8.1 (a) XRD patterns of the SIO NWs at different synthesis temperatures from 770 to 900 °C and (c) the lattice parameter and atomic weight percentage of Sn doped at different synthesis temperatures.

peak appears for 750 ^{o}C grown SIO NWs. When the synthesis temperature is 770 ^{o}C, the intensity of (222) is the highest among others and the FWHM value of ~0.14^{o} is the smallest implying that this temperature is more suitable for the growth of SIO NWs with a good cubic crystal structure. At higher growth temperature such as 900 ^{o}C or higher, the lattice structure becomes poor which maybe due to the Sn^{4+} was vaporized and has taken away from the system through the carrier gas leading the intensity of (222) peak becomes weak. The growth temperatures reported in the previous papers of IO NWs were usually about ~900-1100 ^{o}C[291-292]. Obviously, the doped Sn could effectively decrease the growth temperature of the SIO NWs through the VLS process. According the VLS process, the mixed metal oxide powders, IO and SnO_2 are reducted to metal droplet by graphite at high temperature typically at ~1100 ^{o}C for pure IO. While the mixed powder was heating and processed the reduction reaction, the melting point of In-Sn alloy is ~393 ^{o}C while Sn is less 10 w.t.%[293]. The melting point of this alloy is lower than pure In. Therefore, the Sn dopant would effectively decrease the temperature of the droplet to form which is helpful to decrease the synthesized temperature of the SIO NWs. Furthermore, while the synthesis temperature is getting lower from 900 to 770 ^{o}C, the (222) peak of the SIO NWs was shifted toward higher 2θ value, which is closer to 32^{o} degree as shown in Fig. 8.1(a). The lattice parameter of SIO NWs versus the growth temperature is shown in the Fig. 8.1(c) which indicates that the change in the *a* parameter calculated from the angle shifted of (222) of SIO NWs. The ionic radii of In and Sn are 1.56 and 1.45 Å, respectively[294]. The shift in the diffraction angle of the XRD patterns of nanowires could be due to the diffusion of Sn into the IO lattice sites that leads to the shrinkage of lattice parameters of pure IO. On the other hand additions of SnO_2 to IO form a solid

solution with cubic structure in which Sn^{4+} are substituted for In^{3+}, resulted in the formation of In vacancy to keep the cationanion site relationship of 2:3.

$$3SnO_{2(s)} \xrightarrow{In_2O_3} 3Sn_{In}^{\bullet} + 6O_o + V_{In}^{'''} \quad (8.1)$$

Where $Sn_{In}^{\bullet}$ means Sn substituted for In^{3+} in IO, O_o denotes O at the same oxygen site, and $V_{In}^{'''}$ means a vacancy at a In^{3+} site in the lattice of the SIO NWs. The amount of Sn in the nanowires shown in Fig. 8.1(c) which was measured by EDS analysis is decreased with increasing synthesis temperature increased from 770 to 900 ^{o}C, which is manifested as less-shifted diffraction angle of (222) peak.

The selective growth of the SIO NWs in the Au catalyst film pattern with a diameter of about 100 μm is shown in Fig. 8.2(a). The VLS growth process was carried out at a temperature of 770 ^{o}C for 3.0 hrs under N_2 carrier gas flow rate of 60.0 cm^3/min. Figure 8.2(b) indicates the FE-SEM images of the boxed region shown in Fig. 8.2(a). The clear demarcation demonstrates that the only area defined by the Au catalyst film promotes the synthesis of SIO NWs by the VLS process. Furthermore, the more vertical growth direction SIO NWs are found at the center of the location of the Au pattern as shown in Fig. 8.2(c). The SIO NWs in the edge of the Au pattern [see Fig. 8.2(d)] have random growth direction. The SIO NWs is about 10 μm and the average diameter about 80 nm. The sidewall of the nanowires is very smooth and the geometry of these SIO NWs is uniform. This result is also proved by HR-TEM analysis in the later section. According the high resolution SEM observation, there are some Au catalyst droplets that still adhere on the front of the SIO NWs tips.

The selected area electron diffraction (SAED) pattern of the SIO NWs grown at 770 ^{o}C along [001] axis is shown in Fig. 8.3(a). The indexed

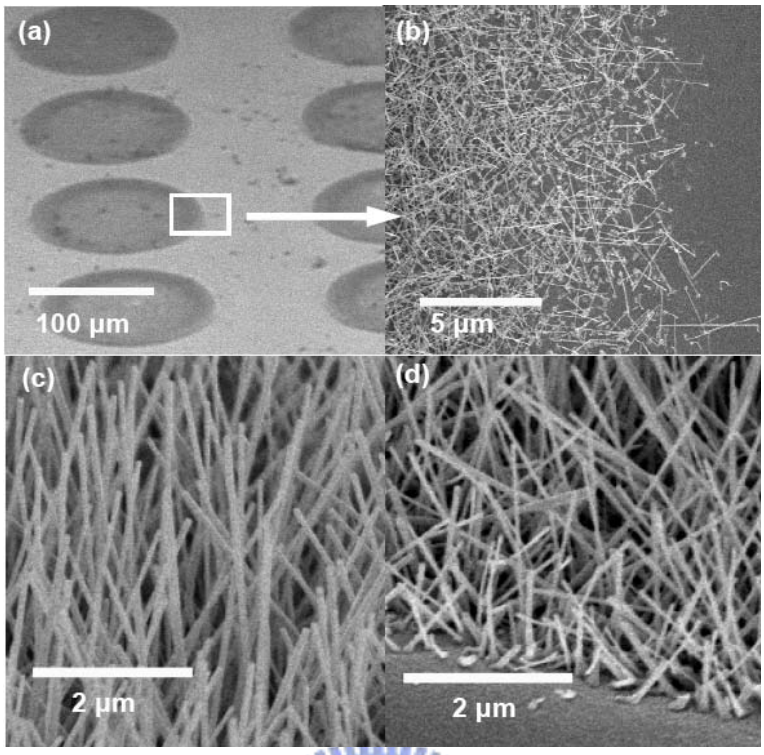

Figure 8.2 FE-SEM images of the SIO NWs : (a) large area of the selective synthesized process of SIO NWs, (b) the zoom in photo of the edge of the 100 μm diameter metal mask for selective growth, (c) 45^{o} tilted view for 10 μm length and ~80 nm diameter of the SIO NWs at central region and (d) is the outside region near the circle of SIO NWs growth.

diffraction patterns corresponding to (200) and (220) indicate that the SIO NWs has a cubic crystalline structure. The clear spots also prove that the SIO NWs are single crystalline structure. After d-spacing calculation, the lattice parameter of the SIO NWs is ~5.19 Å along a-axis which is consistent with the analysis results of the XRD as shown in Fig. 8.1(c). The bright view image indicated in Fig. 8.3(b) shows the geometry and morphology of the SIO NWs. The sidewall of the nanowires is very smooth which agrees with the SEM result. Generally, there is some metal tip remaining which is shown in this image [Fig. 8.3(b)]. The lattice fringes shown in the HR-TEM photograph of the SIO NWs of Fig. 8.3(c) correspond to a cubic structure. The clear contrast of the lattice image indicates the arrangement of In and O in the nanowires. The

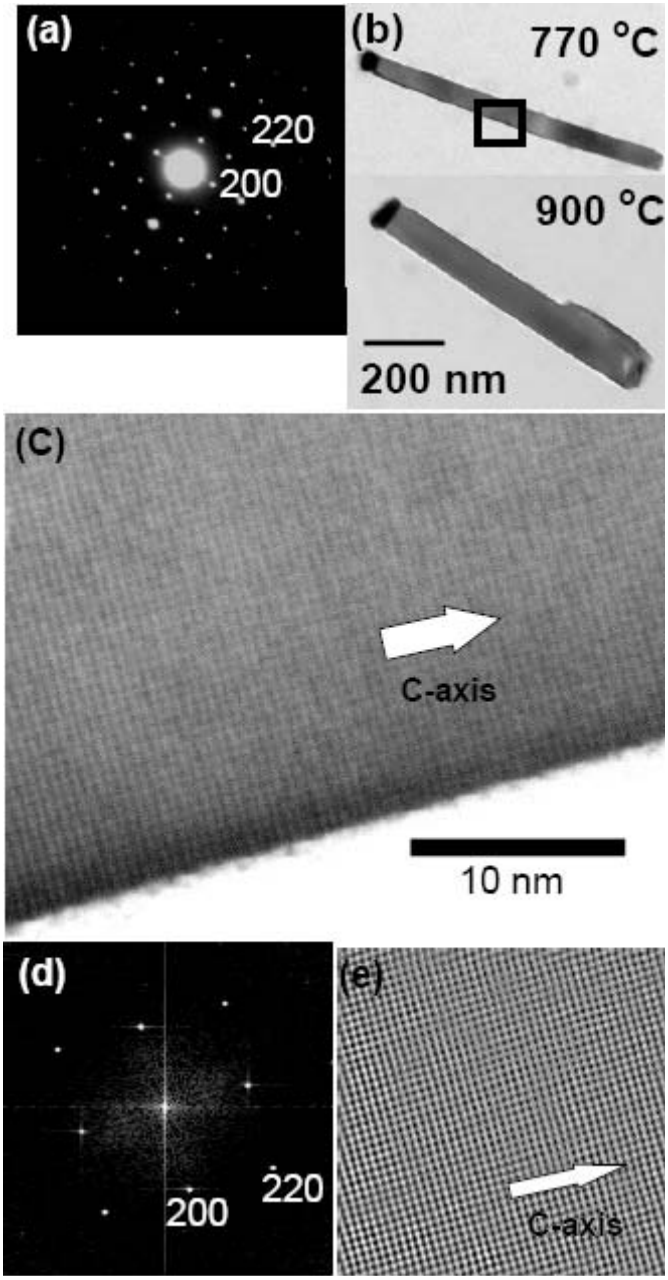

Figure 8.3 TEM photograph of a single crystalline SIO NW : (a) Indexed SAED diffraction indexing pattern, (b) bright view of the SIO NW, (c) HR-TEM image showing the lattice frings, (d) simulated SAED pattern that is consistent with (a), (e) IFFT image for (c).

lattice distance between each fringe is ~5.19 Å along [200] direction. Figures 8.3(d) and (e) depict the computer simulation analysis (Gaton, Inc. DigitalMicrograph^{TM} 3) results of the SIO NWs. Fig. 8.3(d) is the modified pattern of SAED obtained from the transformation of Fig. 8.3(c) using the fast

Fourier Transform (FFT) method. The indexed spots in this pattern are consistent with those in the Fig. 8.3(a), which again proves that the fabricated SIO NWs have a well-defined cubic crystalline structure. The high-resolution image shown in Fig. 8.3(e) is obtained by the inverse fast Fourier transformation (IFFT) of the SAED pattern of Fig. 8.3(a) after removing background noise. The clear lattice fringes along the c-axis in Fig. 8.3(e) are consistent with those in the Fig. 8.3(c) We can obvious produce more clearly atomic images of the NWs [Figs. 8.3(d) and (e)] through the application of simulation tools. It is demonstrated by Fig. 8.3 that the VLS process can be employed to fabricate high quality SIO NWs that have well-defined cubic crystalline structure and less lattice defects.

The high-resolution EDS spectrua (Figs. 8.4) indicate the constituent elements and the chemical composition of the SIO NWs grown at 770 ^{o}C. There are three clear peaks of In that has been easily detected and some other elements have also been found. The clear In and O peaks located at ~3.5 keV (main peak) and ~0.65 keV, respectively can indicate the composition of the nanowires. Through the semi-quantitative analysis, the chemical composition of In/O of the SIO NWs is about 0.38/0.59 by atomic weight percent ratio. Furthermore, according to the EDS spectrum as shown in Fig. 8.4(b), weak peak located at ~1.75 keV is identified as Sn. The doped amount of Sn is ~2.45 a.t.% after the quantitative analysis of this spectrum. That means the VLS process can offer good control for the chemical composition for the fabricated SIO NWs. On the other hand, the Cu signal comes from the TEM copper grid holder. The Au signal has been detected from the tip in front of the SIO NWs. This result demonstrates that the Au catalyst remains through out the VLS process.

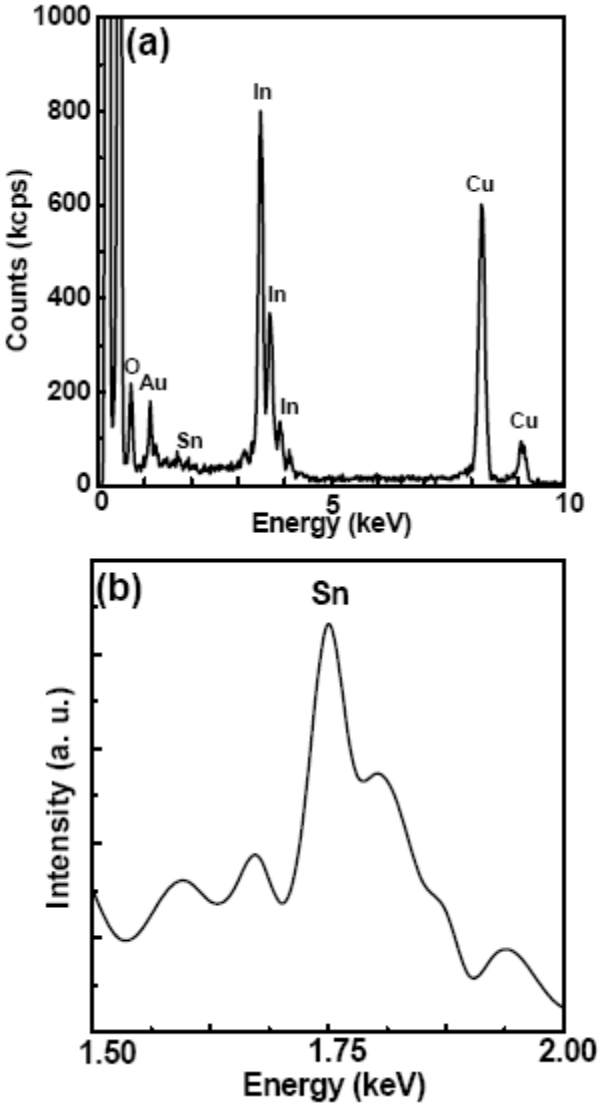

Figure 8.4 (a) EDS spectra indicating the elements In, O , and Sn distributions of the SIO NWs, (b) EDS spectrum of Sn peaks of the SIO NWs grown at 770 ^{o}C.

The XPS spectra is shown in Fig. 8.5(a) depict the full region scanned from 0 to 1200 eV with respect to two different areas of the same Si substrate in which one is the spectrum (1) and the other is the bare Si surface without patterning SIO NWs in Au patterned surface [spectrum (2)]. When the electron beam focuses on patterned surface in which the SIO NWs exist, it indicates that some elements, such as C, O, Si, In_{3p}, In_{3d}, In_{4p}, In_{4d} and Sn_{3d} can be clearly detected in this area as observed in XPS spectrum (1) of Fig. 8.5(a). This result

further proves the selective growth process of the SIO NWs in our experiment. High resolution scanned informations provided in Figs. 8.5(b), (c), and (d) are for the separated analysis of elements, O, In, and Sn, respectively. The high resolution XPS spectrum of the O_{1s} signal [Fig. 8.5(b)] indicates that the binding energy is ~529.6 eV that is consistent with that of O_{1s} in In_2O_3. Furthermore, another O_{1s} peak, 533.5 eV is indicating that less Sn bonded with O while Sn^{4+} diffuses into the nanowires. Figure 8.5(c) indicates the peaks of ~452.3 eV for $3d_{3/2}$ and ~445.6 eV for $3d_{5/2}$ of In, respectively. The $3d_{3/2}$ and $3d_{5/2}$ in Fig. 8.5(d) are marked as ~495.4 eV and ~486.3 eV that represent the Sn dopant diffused into those nanowires through the fabricated process. For different growth temperatures from 770 to 900 ^{o}C, the amount of Sn doped decreases from 2.45 to 0.83 atomic weight percent with increasing synthesized temperature as shown in Fig. 8.1(b). These spectral information of 770 ^{o}C synthesized are calculated by analytical process. The atomic weight percentages of In, Sn and O at 770 ^{o}C grown nanowires are ~38.6 %, ~2.43 %, and ~58.8 %, respectively, based on the calculation from the XPS spectra, which are in good agreement with those analyzed from the EDS measurements.

The room temperature photoluminescence (PL) spectra of the SIO NWs grown at various temperatures from 770 to 900 ^{o}C are shown in Fig. 8.6. It is well known that the bulk In_2O_3 just can emit very weak light at room temperature. However, a stronger and sharper PL emission spectrum from the SIO NWs is shown in the present study. Under the excited wavelength of 260 nm of Xe lamp, a broadened optical emission spectrum located at ~400-460 nm has been found, in which four distinct peaks can be easily observed; one is at ~425 nm which originated from Si(100) substrate, while the others excited by the SIO NWs are located at 416, 440, and ~446 nm. Based on previous

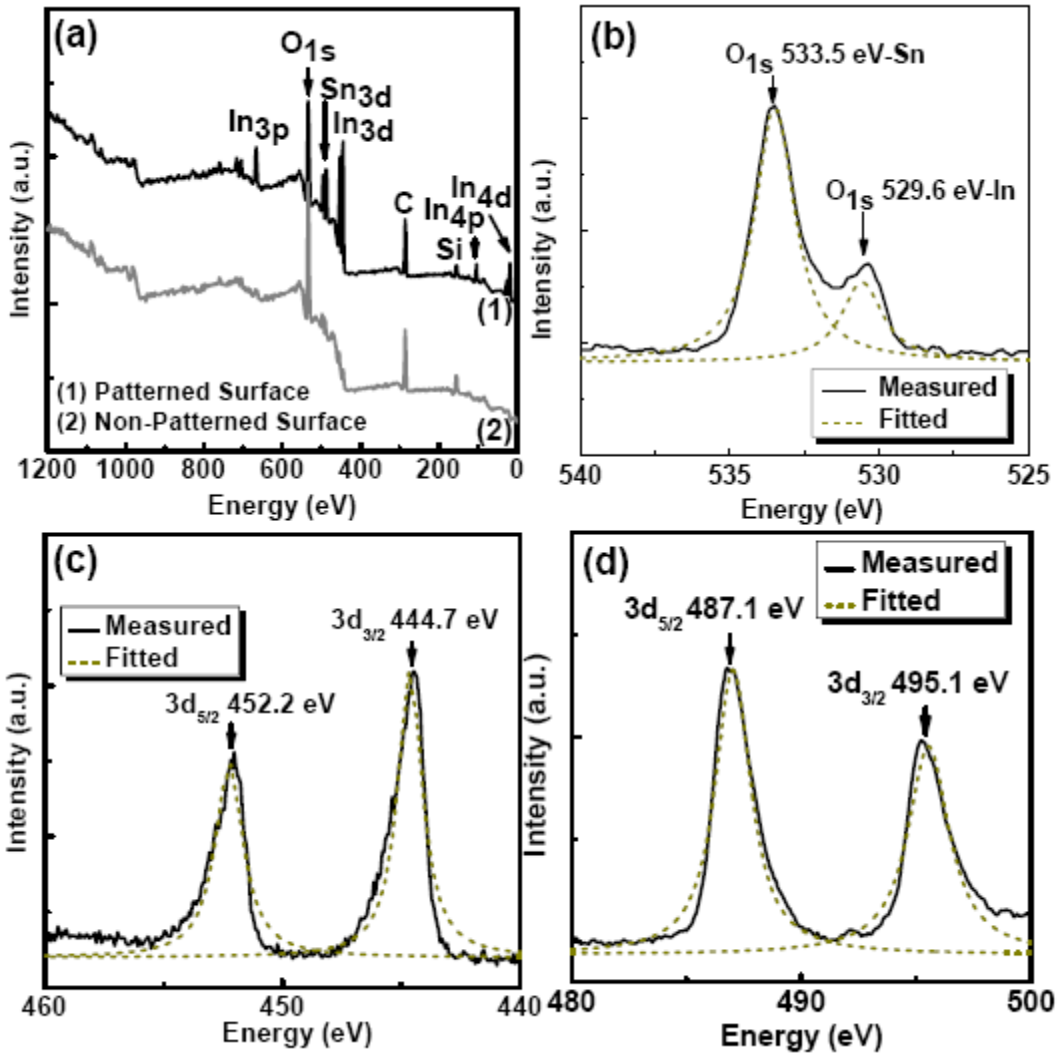

Figure 8.5 XPS spectra of the SIO NWs: (a) fully scanned from 0 to 1200 eV, (b) high resolution selective spectrum of O, (c) high resolution selective spectrum of In, and (d) high resolution selective spectrum of Sn, respectively.

Reports[295-296], the strong PL emission of the IO NWs was located at ~416 nm. The strongest PL emission peak of the SIO NWs in the present study is located at 440 nm instead of 416 nm (Fig. 6) which reveals the optical band gap of ~2.82 eV. As the Sn is doped into IO NWs, the main emitted peak shifts toward the longer wavelength, indicating that the Sn addition would create new separated band gap levels (E_g) of SIO NWs. The difference in energy between these levels is smaller than that in IO NWs, which can result in longer wavelength emission. Such E_g lowering can be attributed to the formation of

localized band edge states due to charge exchange and structural relaxation, and is proportional to the orbital energy and the size difference between atoms of the elements. The blue emission located at 440 nm occurred can be explained by the following step. An electron in donor level is captured by a hole on an acceptor (V_{In} and V_{Sn}) become a radiative recombination center to emit blue light, that is, the creation of vacancies due to the addition of Sn is the cause of the mean emission of the SIO NWs at 440 nm instead of 416 nm. Furthermore, the higher fabrication temperatures ranging from ~800 to 900 ^{o}C can prompt the main emission peak to shift to longer wavelength (440 to 446 nm) because at the higher temperature process, metal vacancies such as V_{In} or V_{Sn} would increase speedily that will cause longer wavelength emitted. The appearance of an upper tail at 475 nm of the PL spectrum (Fig. 8.6) indicates the ionized oxygen vacancies, $V_O^{\bullet}$ or $V_O^{\bullet\bullet}$, that contribute to some new energy levels in the band gap of the SIO NWs.

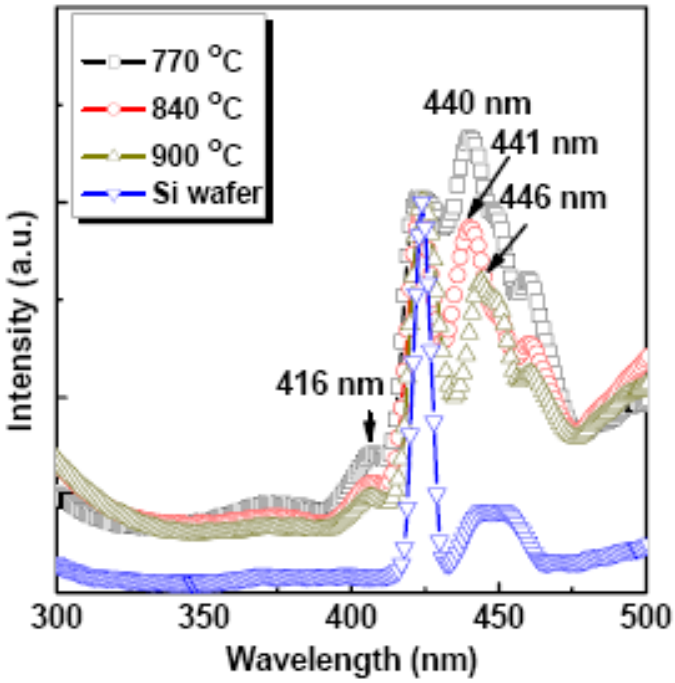

Figure 8.6 Emission spectra of the SIO NWs using 275 nm incident Xe lamp at room temperature (298 K).

The field emission (FE) characteristics of the SIO NWs grown at 770 ^{o}C and 900 ^{o}C are shown in Fig. 8.7, indicating that their I-V characteristics follow a Fowler-Nordheim (F-N) behavior. The F-N plots in the inset of Fig. 8.7 where $log(I^2/V)$ is plotted as a function of $1/E$ are characterized by two constant slopes for two different synthesized temperatures. The turn-on electric field of SIO NWs grown at 770 ^{o}C is ~0.66 V/μm at 1.0 mA/cm^2 and its field emission enhancement coefficient, β is 1.48×10^5. On the other hand, as the grown temperature is raised to 900 ^{o}C, the turn-on electric field and the β value are ~0.78 V/μm and 0.84×10^5, respectively. Such an increase in the turn-on electric field and decrease in the β value may be attributed to poor crystallinity of the SIO NWs grown at higher temperatrue. Furthermore, in comparison with other nanowires such as CNTs[297,298,301], ZnO NWs[299,300,302] amd IO[303] NWs listed in Table 1, our SIO NWs have lower turn-on electric field and larger enhancement factor, β than IO[304]. This difference can be attributed to the Sn doped into the IO NWs, which result in the increase of the conductivity and consequently leading to lower the turn-on electric field and enhance the β value of the NWs.

The resistances of the SIO NWs grown at different temperatures are shown in Fig. 8.8. The saturation of the field emission current occurs in 770 and 900 ^{o}C grown SIO NWs. Each SIO NWs has its own highest resistance at below the turn-on electric-field. The drop of voltage across such a resistor would decrease the effective applied voltage, and therefore causes a flattening of the characteristics occurred[17]. After fitting to the low emission current part of the measured data, the resistances corresponding to 770 ^{o}C and 900 ^{o}C grown SIO NWs are 18.3, and 27.5 kΩ , respectively. The decrease in resistance is proportional to the increase in Sn dopant concentration which means the lower growth temperature the more amounts of Sn dopant diffusion. The lower

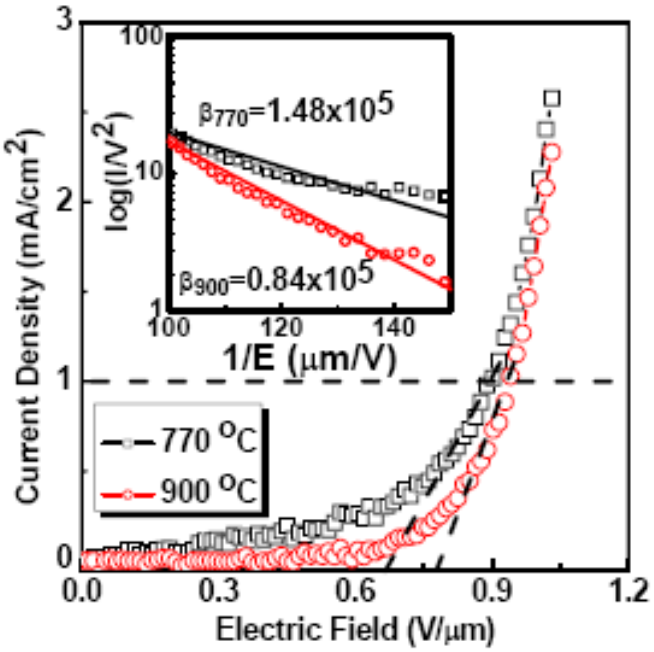

Figure 8.7 Field emission characteristic of the SIO NWs and the inset is the F-N plot that is calculated from field emission enhancement coefficient.

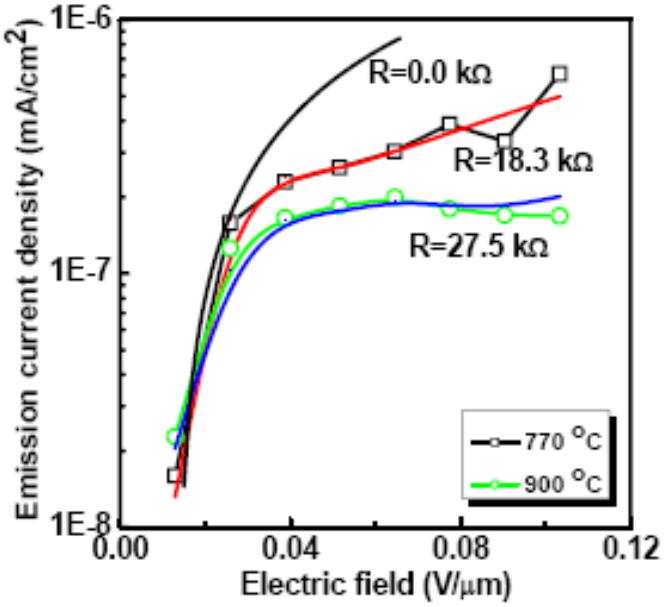

Figure 8.8 Emission current density versus lower electric field of the different temperature 770 and 900 ^{o}C grown SIO NWs.

resistance occurred in 770 ^{o}C grown SIO NWs which have larger amount of Sn dopant may be attributed to the Sn-enhanced electron density and higher concentration of In vacancies [Eqn. (8.1)]. Furthermore, the field-adjustment factor, α is an index to determine the ability to enhance local field from the field emission tips. In this study, α value of the synthesized temperature which is located at 770 ^{o}C and 900 ^{o}C grown nanowires are 2.34×10^{-4} and 2.29×10^{-4}, respectively, indicating that the SIO NWs synthesized at 770 ^{o}C have larger α value than those grown at 900 ^{o}C. In fact, the better crystal structure of SIO NWs grown at 770 ^{o}C effectively develops the α value because less impurity and defect will help the free electrons emission mechanism under the low electric field. This result can be also explained that the more vertical the growth of the tips of the SIO NWs, the better the ability to enhance local electric field.

On the basis of the field emission characteristics of oxide NWs and CNTs displayed in Table 8.1, the turn-on electric field is effectively decreased by the Sn dopant for those NWs. The turn-on electric field is decreased 4 times and the β value is enhanced 2 orders due to the Sn doped into IO NWs. In the meanwhile, with the same Sn doped level (~2.45 a.t.%), the SIO NWs have lower series resistance than the SZO NWs that would enhance the stability of the emission current. Besides, the SIO NWs have lower synthesized temperatures than the SZO NWs which have better opportunity to easily integrate into the semiconductor technology. As for the comparison between CNTs and oxide NWs, most of oxide NWs have lower turn-on electric field than CNTs, but CNTs have lower synthesized temperatures as listed in Table. 8.1

Table 8.1 The field emission characteristics of carbon nanotubes (CNTs) and oxide NWs with and without Sn doped.

	E_{to} (V/μm)	J_{to} (mA/cm^2)	β	R_s (kΩ)	T_{growth} (^{o}C)	Reference
CNTs	**1.4**	**10-30**	**10,600**	**N/A**	**500**	**13**
CNTs	**1.5-4.5**	**0.01-0.1**	**1000-3000**	**N/A**	**N/A**	**14**
CNTs	**4.0**	**2.0**	**1,500**	**N/A**	**750**	**18**
ZnO NWs	**0.83**	**1.0**	**7,180**	**85.43**	**900**	**15**
ZnO NWs	**0.7**	**1.0**	**40,000**	**N/A**	**1100**	**16**
SZO NWs	**0.15**	**1.0**	**445,000**	**24.52**	**820**	**19**
IO	**2.7**	**10^{-3}**	**1600**	**N/A**	**950**	**20**
SIO NWs	**0.68**	**1.0**	**148,000**	**18.3**	**770**	**Present work**

Where E_{to} is turn-on electric field, J_{to} turn-on current density, β field emission enhancement factor, R_s turn-on series resistance, and T_{growth} synthesized temperature.

8.4 Summary

In summary, the SIO NWs is successfully fabricated by VLS process while the added Sn dopant that effectively decreases the synthesis temperature from ~1100 ^{o}C to ~770 ^{o}C. The geometry and morphology (80 nm diameter and ~10 μm length) of the SIO NWs are very perfect without much contamination. On the basis of the fabricated process, these nanowires have well-defined cubic crystal structure and less defect or dislocation. On the other hand, the SIO NWs emitted a strong blue light band at ~445 nm at room temperature by using a

Xe-lamp (275 nm) as the excitation source. Furthermore, the doped Sn also could shift the main emission to shorter wavelength of the SIO NWs. Therefore, the synthesis of SIO NWs would possess technological promise for manipulating the nano optical properties, which is important in nanoscale optoelectronic applications. The field emission measurements indicated the low turn-on electric field of 0.66 V/μm at a current density of 1.0 mA/cm^2. The low temperature fabricated (~770 ^{o}C) SIO NWs exhibited higher field emission area factor of about 1.48×10^5 and larger field adjustment factor of 2.34×10^{-4} than those values of 900 ^{o}C fabricated nanowires, which is due to the Sn dopant that remained more into the nanowires when fabricated at 770 ^{o}C. The Sn dopant added in the in SIO NWs is ~2.45 a.t.% which lower the resistance and increase the conductivity, respectively. Using these structurally controlled Sn doped SIO NWs, a more interesting physical and chemical properties can be studied. Therefore, the vertically and selectively grown SIO NWs array is a good candidate for the future flat panel display applications.